

Dipole-Promoted and Size-Dependent Cooperativity between Pyridyl-Containing Triazolophanes and Halides Leads to Persistent Sandwich Complexes with Iodide

Yongjun Li,[†] Maren Pink, Jonathan A. Karty, and Amar H. Flood*

Department of Chemistry, Indiana University, Bloomington, 800 East Kirkwood Avenue, Bloomington, Indiana 47405

Received September 30, 2008; E-mail: aflood@indiana.edu

Encapsulation of a guest by the cooperative dimerization of a host to form “sandwich” complexes is an effective means to increase dimensionality¹ for optimizing complex stability. Lessons provided by crown ether binding with alkali metals² indicate the importance of a size difference between an ion and the cavity of the receptor for forming sandwiches. This mismatch provides a means to decrease the stability of the 1:1 complex (K_1) relative to the 2:1 (K_2). The relative magnitudes of K_1 and K_2 thereby provide insights into cooperative effects.³ Only a few 2:1 sandwich complexes are known for anionic guests. Here, the 1:1 and 2:1 complexes are observed either depending upon the stoichiometry in solution⁴ or solely as 2:1 complexes in the solid state.⁵ Only an “anti-crown” mercuracarborand⁶ shows only 2:1 sandwiches in solution with halides; however, the binding constants were not characterized. Cooperativity has been quantified⁴ in two instances to result from interactions between receptors. Here we present findings on a new class of triazolophane⁷ incorporating pyridyl ring systems (Figure 1) that forms strong and persistent 2:1 complexes with the large I^- ion in solution. Quantitative binding studies with F^- , Cl^- , and Br^- show both 2:1 and 1:1 complexes implicating the importance of the electronic character of the cavity in modulating cooperativity.

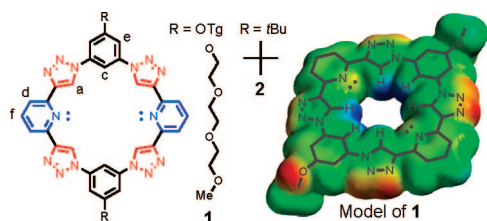


Figure 1. Representations of pyridyl-containing triazolophanes **1** and **2**, and the electrostatic potential surface of a model of **1** (blue sections represent regions of positive electrostatic character).

Prior studies on tetraphenylene-based triazolophanes^{7,8} show size-dependent 1:1 binding with halides ($Cl^- > Br^- > F^- \gg I^-$), using only $CH\cdots X^-$ hydrogen bonding,⁹ and a propensity for self-association. Molecular modeling indicated the I^- ion was not fully encapsulated. This tendency could lead² to dimerization-induced binding of iodide ions, yet the 2:1 complexes were not observed. To elaborate on this idea, pyridyl ring systems were considered as a replacement for the phenylenes. Pyridines have been used previously^{8b,10} to alter the electronic character and size of binding sites. Consequently, compounds **1** and **2** were designed with pyridyl rings replacing the C-linked phenylenes in the west and east directions. Modeling (HF/3-21G) confirms the predictions: Pyridyls generate negative electrostatic potentials inside the cavity (Figure 1) and the cavity becomes oval (the vertical axis gets smaller by ~ 0.3 Å and the horizontal axis increases by > 0.2 Å). We

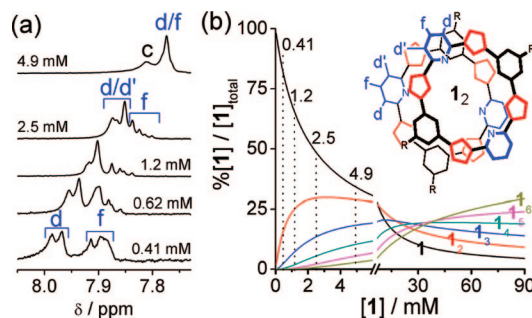


Figure 2. (a) 1H NMR spectra of **1** (pyridyl region) as a function of concentration (CD_2Cl_2 , 298 K, 400 MHz) and (b) calculated speciation curves for self-association up to the hexamer **1**₆ with $K_E = 255 M^{-1}$

hypothesize that the cumulative effect of these features will destabilize the 1:1 complex in favor of the 2:1 sandwich.

The triazolophanes were prepared following prior methods⁷ of symmetric chain extension followed by macrocyclization under conditions of high dilution and Cu(I) catalysis. The electrospray ionization mass spectrometry (ESI-MS) and 1H NMR spectra confirm¹¹ the identity of the triazolophane.

Triazolophane **2** was only soluble as the tetrabutylammonium (TBA) salt: $[2_2 \cdot I^-]TBA$. Crystals grown for X-ray analysis diffract weakly. A partial solution¹¹ shows (a) formation of the 2:1 sandwich with the I^- ion located between both triazolophanes, (b) the triazolophanes within π stacking distance (3.4 Å), and (c) that the angle of rotation (θ) between the two triazolophanes is $\sim 56^\circ$.

The triazolophane **1** was examined in dichloromethane for its propensity to self-associate using both 1H NMR (Figure 2) and UV studies.¹¹ The aromatic protons shift upfield with concentration (0.4–90 mM) indicating π -stacking and leading to the self-association constant,¹¹ $K_E = 255 \pm 70 M^{-1}$. Consistently,^{7b} continual changes in the diffusion coefficient¹¹ are observed from 2 to 100 mM. Modeling¹² of the equilibria shows that with increasing concentration (Figure 2b), the amount of monomer decreases and the dimer shows a maximum in its population at ~ 3 mM, thereafter, both species are replaced by higher order species. The splitting pattern in the pyridyl region of the 1H NMR spectra (Figure 2a) agrees with this picture. At 0.41 mM, the pyridyl H^d and H^f protons are observed to form an A_2X spin system corresponding to the monomer **1**. This pattern transforms into an ABC spin system at 2.5 mM, which can arise when the two H^d protons are no longer equivalent as expected (inset, Figure 2b) from a rotated ($0^\circ < \theta < 90^\circ$), π -stacked pair of triazolophanes, **1**₂. A doublet of doublets (H^f) sits upfield from the partially overlapping doublets of the inequivalent H^d and $H^{d'}$ protons. At 4.9 mM, a broad singlet replaces the ABC pattern indicating a shift to rapidly equilibrating higher-order aggregates. The UV spectra of **1** (2 μM –1 mM) show a decrease in the normalized intensities consistent with self-association.^{7b} We attribute the rotated configuration in **1**₂ to

[†] Present address: CAS Key Laboratory of Organic Solids, Institute of Chemistry, CAS, Beijing, 10080, P. R. China.

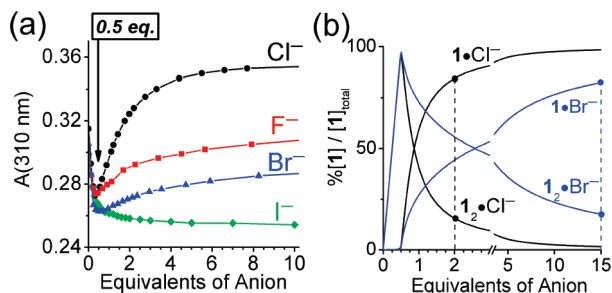


Figure 3. (a) UV binding curves for **1** (20 μM) with halides (CH₂Cl₂, 298 K) and (b) the speciation curves calculated¹² from K_1 and K_2 (Table 1) for Cl⁻ and Br⁻ at 5 mM.

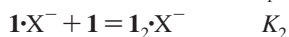
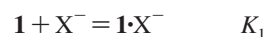
electrostatic complementarity between the opposite dipoles on the pyridines (−2.4 D) and the triazoles (+5.0 D) of the triazolophane dimer pair.

Halide binding was investigated using UV titration (Figure 3a). Upon addition of F⁻, Cl⁻, and Br⁻ to **1** (20 μM) the absorbance decreases to a minimum at 0.5 equiv as a consequence of the π -stacked structure in the 2:1 complex. The absorbance then increases with the addition of more halide leading to the 1:1 complex. For I⁻, the peak intensity decreases continuously during the titration. When repeated at 1 μM,¹¹ addition of F⁻, Cl⁻, and Br⁻ appears to proceed directly to the 1:1 complex while only I⁻ forms the 2:1 sandwich.

Table 1. Binding Energies (kcal mol⁻¹, ±10%) between **1** (20 μM) and the TBA Halides in CH₂Cl₂ Determined by Equilibrium-Restricted Factor Analysis of UV Titration Data

	ΔG_1 (K_1/M^{-1})	ΔG_2 (K_2/M^{-1})	ΔG (β_2/M^{-2})
F ⁻	−7.4 (275 000)	−7.6(380 000)	
Cl ⁻	−8.5(1 600 000)	−7.2(190 000)	
Br ⁻	−7.5 (315 000)	−7.9(580 000)	
I ⁻			−14.9(8.6 × 10 ¹⁰)

Quantitative analysis of the UV titration data was conducted using an equilibrium-restricted factor analysis¹³ of the entire wavelength range¹¹ to characterize the binding constants (Table 1). The models used the stepwise formation equilibria



or the direct formation of the sandwich complex



For the I⁻ ion, the best fit was obtained from the direct formation of the 2:1 dimer (β_2) at both concentrations. At the higher concentration, the titration data for F⁻, Cl⁻, and Br⁻ are best fit with the stepwise equilibria (K_1 and K_2): The data obtained from the 20 μM titration contains reasonable proportions of all three absorbers, **1**, **1**₂•X⁻ and **1**•X⁻, and is under moderate binding conditions,¹⁴ therefore, it is more accurate than fitting the data at either lower (1 μM) or higher (5 mM, NMR) concentrations. The accuracy of these models was confirmed by inspecting the speciation curves calculated¹¹ from the K_1 , K_2 , and β_2 values. At 1 μM, these curves confirm that the 2:1 complex is present at <10%, consistent with its apparent absence in the fitting.

The relative values of K_1 and K_2 , as well as the behavior of I⁻, indicate³ that positive cooperativity follows the order I⁻ ≪ Br⁻ < F⁻ whereas Cl⁻ displays negative cooperativity. The halides were defined as having two identical binding sites and the triazolophane with one binding site. Statistical binding would occur if $K_2 = K_1/4$ and deviations higher or lower signify positive and negative

cooperativity, as observed. These cooperative effects were verified graphically utilizing linear Scatchard plots.^{11,15}

The 2:1 complex **1**₂•I⁻ is persistent in solution. To estimate the stepwise binding constants, speciation curves¹¹ were generated¹² for K_1 values while keeping β_2 constant. The NMR concentration of 2 mM was used to provide the greatest opportunity of observing the 1:1 complex. This approach generates upper and lower limits: $K_1 < 3200$ and $K_2 > 32\,000\,000\,M^{-1}$. The former concurs with the K_1 value (5000 M⁻¹) for the related tetraphenylene triazolophane.^{7b}

Solution structures of **1** with halides were characterized (Figure 4) by ¹H NMR spectroscopy (CD₂Cl₂, 400 MHz). While different chemical shift behaviors are observed for the various halides, each follows the calculated¹¹ speciation curves ([**1**] = 5 mM). Upfield and downfield shifts are attributed to the relative importance of π -stacking and halide binding, respectively. In the simplest case, titration of **1** with TBAI (Figure 4a) displays shifts in all positions up to the addition of 0.5 equiv consistent with 2:1 stoichiometry, **1**₂•I⁻, as confirmed by a Job's Plot.¹¹ The stability of the sandwich complex is maintained in the presence of 150 equiv of I⁻. The inner triazole (H^a) and phenylene (H^c) CH protons both shift downfield by ~0.2 ppm indicating the dominance of I⁻ binding on their positions.^{7b} The outer protons on the pyridyl rings (H^d and H^f) shift modestly downfield while the phenylene H^e moves slightly upfield, showing the importance of π -stacking. Diffusion NMR is consistent with sandwich formation. Addition of 0.5 equiv of I⁻ steps the diffusion coefficient from 3.5 to 3.4 × 10⁻¹⁰ m² cm⁻¹ where it stays up to 3 equiv.

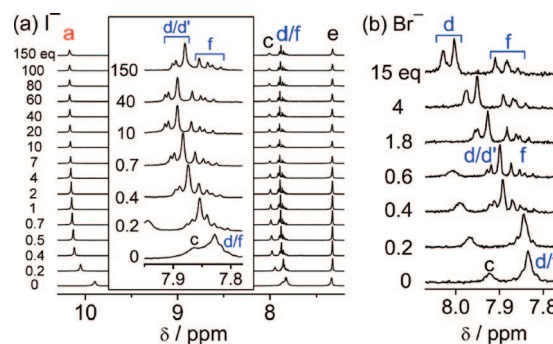


Figure 4. ¹H NMR spectra showing the titration of **1** (5 mM, CD₂Cl₂, 400 MHz, 298 K) with (a) I⁻ (inset, pyridyl region) and (b) Br⁻ (pyridyl region).

The solution structure of **1**₂•I⁻ is consistent with dimer **1**₂ and the preliminary crystal structure of [**2**₂•I]TBA. An ABC spin system for the pyridyl protons (inset, Figure 4a) indicates two rotated face-to-face triazolophanes. In support of this geometry, a ¹H–¹H ROSEY experiment shows through-space cross peaks from (a) the phenylene H^e and (b) both the α- and β-methylene protons on the OTg substituent to the pyridyl H^d and H^f protons. In the parent triazolophane, the distances are too large (>6.4 Å) to support an NOE. These observations indicate an average solution structure with a centrally located halide.

The TBACl and TBABr salts behave the same as TBAI up to ~0.5 equiv (e.g., Br⁻, Figure 4b). Further additions indicate the shift from 2:1 to 1:1 complexes with the ABC spin system becoming replaced by the A₂X system. The relative intensities of these two spin patterns signify the population ratio between the 2:1 and 1:1 species. The point where the A₂X system dominates occurs at 2.0 equiv for the Cl⁻,¹¹ whereas for the Br⁻ it is as late as 15 equiv, perfectly consistent with the differences in the speciation curves (Figure 3b, dashed lines) between these two halides.

In the case of TBAF, the titration behavior shows¹¹ a cross over to the A_2X system beyond 22 equiv. The *shifts* in the proton signals, however, are more complicated than in the Cl^- and Br^- cases. Beyond 0.5 equiv all the proton signals except H^c shift steadily upfield. The upfield shifts normally indicate increasing self-association. Molecular modeling (HF/3-21G)¹¹ indicates that in the 1:1 complex $1 \cdot F^-$, all six CH H-bond donors bind symmetrically with the F^- ion. Consequently, the proton shifts that occur upon transformation into the 1:1 complex are attributed to the conformational changes of **1** in addition to the effects of halide binding and dedimerization.

Complex formation was confirmed by ESI-MS. The ESI-MS is often taken to reflect the solution species present in solution.⁴ The analysis¹¹ of solutions ($[1] = 50 \mu M$, CH_2Cl_2) with 2 equiv of Cl^- showed the peak for the 1:1 complex stronger than the 2:1. For the Br^- , the two peaks were equal. Under these conditions, the I^- sample retained the dominance of its 2:1 dimer peak. These observations agree with the calculated speciation curves¹¹ and the change from negative (Cl^-) to positive cooperativity (Br^- , I^-). A competition experiment for halide binding with **1** was conducted, in which a solution containing all four halides at 0.125 equiv was analyzed. The peak intensities indicate the relative stabilities of the sandwiches: $I^- \gg Br^- > Cl^-$. The F^- complexes were not observed. In the same spectrum, the 1:1 peaks followed $Cl^- > Br^- \approx I^-$. These observations again concur with the speciation curves.

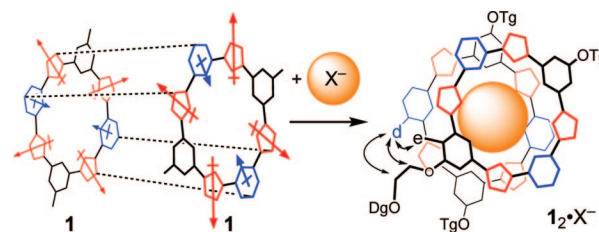
All of the titration data validate the accuracy of the K_1 , K_2 , and β_2 values and the presence of cooperativity. The propensity for 2:1 halide binding by the pyridyl triazolophanes can be best explained by comparison to the tetraphenylene ones.^{7b} For the Cl^- and Br^- ions, the ΔG_1 values for **1** are 0.5 and 0.9 kcal mol⁻¹ lower, respectively, than for the tetraphenylenes.^{7b} Modeling (HF/3-21G)¹¹ shows both 1:1 complexes are planar with the halides fitting snugly inside the cavity. These observations confirm our hypothesis that the lone pairs of electrons on the nitrogens are acting in a destabilizing way. The fact that the 1:1 Br^- complex is more greatly affected is consistent with its larger size and therefore closer proximity to the nitrogen lone pairs.

In the case of F^- , the 1:1 complex is more stable by 0.3 kcal mol⁻¹, which is consistent with the centrally located F^- ion in **1**: Being able to engage with six CH H-bond donors rather than three, as is the case for tetraphenylenes,^{7b} more than overcomes the repulsions from the pyridyl nitrogens. The K_2 value has been measured^{13b} for a related tetraphenylene-triazolophane at -6 kcal mol⁻¹, which indicates that the 2:1 sandwich dimer has in fact gained in strength by ~ 1.5 kcal mol⁻¹ for **1**.

Lastly, I^- binding shows highly positive cooperativity. In contrast to the smaller halides, modeling (HF/3-21G) of the 1:1 complex shows¹¹ the iodide ion to be less encapsulated in $1 \cdot I^-$, relative to the tetraphenylene. This structural feature is a hallmark² for favoring sandwich complexes. A calculation on the 1:1 complex shows that the negative electrostatic potentials on the pyridyls are retained in the presence of the I^- ion. The increase in K_2 , therefore, must stem from the novel configuration of the π -stacked and rotated pair of triazolophanes: Registration between opposite dipoles (pyridine and triazole), which guides the angle of rotation between dimers, also aids in partially extinguishing (Scheme 1) the pyridyl-based repulsions in the 2:1 sandwiches.

The smaller halides fit snugly inside the cavity and they all have similar 2:1 binding strengths (Table I). Consequently, the dipole-stabilized dimers must be primarily responsible for their sandwich formation. Positive cooperativity is seen (F^- , Br^-) when the 1:1 binding strength is not significant enough to overcome the dimer's affinity. The F^- is too small and the Br^- too large for favorable

Scheme 1. Representations of the Opposite Dipoles Participating in the Formation of $1_2 \cdot X^-$ ^a



^a NOE cross peaks are labeled in $1_2 \cdot X^-$.

1:1 complexes. The Cl^- has large 1:1 binding strength to offset the dimer leading to slight negative cooperativity.

In conclusion, pyridyl units destabilize the 1:1 triazolophane complexes on account of the $N:\cdots X^-$ electron pair repulsions. In the 2:1 sandwich complexes, the repulsions become reduced by partial cancellation of opposite dipoles. This phenomenon can only occur in the π -stacked dimers. These elements lower K_1 and increase K_2 turning on cooperativity. The size matching between F^- , Cl^- , and Br^- and the central cavity leads to modest cooperative effects. However, when these factors are coupled to a large size mismatch, highly positive cooperativity leads to the enhanced stability and persistent nature of the I^- sandwich complex.

Acknowledgment. The authors thank D. A. Vander Griend for discussions.

Supporting Information Available: Synthesis, characterization, titration, modeling, ESI-MS, and X-ray analyses. This material is available free of charge via the Internet at <http://pubs.acs.org>.

References

- (1) (a) Hof, F.; Craig, S. L.; Nuckolls, C.; Rebek, J. *Angew. Chem., Int. Ed.* **2002**, *41*, 1488–1508. (b) Kang, S. O.; Hossain, M. A.; Bowman-James, K. *Coord. Chem. Rev.* **2006**, *250*, 3038–3052.
- (2) Bajaj, A. V.; Poonia, N. S. *Coord. Chem. Rev.* **1988**, *87*, 55–213.
- (3) (a) Ercolani, G. J. *Am. Chem. Soc.* **2003**, *125*, 16097–16103. (b) Badjic, J. D.; Nelson, A.; Cantrill, S. J.; Turnbull, W. B.; Stoddart, J. F. *Acc. Chem. Res.* **2005**, *38*, 723–732.
- (4) (a) Choi, K. H.; Hamilton, A. D. *J. Am. Chem. Soc.* **2001**, *123*, 2456–2457. (b) Choi, K. H.; Hamilton, A. D. *J. Am. Chem. Soc.* **2003**, *125*, 10241–10249. (c) Kubik, S.; Goddard, R.; Kirchner, R.; Nolting, D.; Seidel, J. *Angew. Chem., Int. Ed.* **2001**, *40*, 2648–2651. (d) Rodriguez-Docampo, Z.; Pascu, S. I.; Kubik, S.; Otto, S. *J. Am. Chem. Soc.* **2006**, *128*, 11206–11210.
- (5) (a) Hossain, M. A.; Llinares, J. M.; Powell, D.; Bowman-James, K. *Inorg. Chem.* **2001**, *40*, 2936–2937. (b) Custelcean, R.; Remy, P.; Bonnesen, P. V.; Jiang, D. E.; Moyer, B. A. *Angew. Chem., Int. Ed.* **2008**, *47*, 1866–1870.
- (6) (a) Lee, H.; Diaz, M.; Knobler, C. B.; Hawthorne, M. F. *Angew. Chem., Int. Ed.* **2000**, *39*, 776–778. (b) Lee, H.; Knobler, C. B.; Hawthorne, M. F. *J. Am. Chem. Soc.* **2001**, *123*, 8543–8549.
- (7) (a) Li, Y.; Flood, A. H. *Angew. Chem., Int. Ed.* **2008**, *47*, 2649–2652. (b) Li, Y.; Flood, A. H. *J. Am. Chem. Soc.* **2008**, *130*, 12111–12122.
- (8) Also see related foldamers: (a) Juwarker, H.; Lenhardt, J. M.; Pham, D. M.; Craig, S. L. *Angew. Chem., Int. Ed.* **2008**, *47*, 3740–3743. (b) Hecht, S.; Meudtner, R. M. *Angew. Chem., Int. Ed.* **2008**, *47*, 4926–4930.
- (9) (a) Farnham, W. B.; Roe, D. C.; Dixon, D. A.; Calabrese, J. C.; Harlow, R. L. *J. Am. Chem. Soc.* **1990**, *112*, 7707–7718. (b) Zhu, S. S.; Staats, H.; Brandhorst, K.; Grunenberg, J.; Gruppi, F.; Dalcanele, E.; Luetzen, A.; Rissanen, K.; Schalley, C. A. *Angew. Chem., Int. Ed.* **2008**, *47*, 788–792. (c) Hay, B. P.; Bryantsev, V. S. *Chem. Commun.* **2008**, 2417–2428. (d) Yoon, D. W.; Gross, D. E.; Lynch, V. M.; Sessler, J. L.; Hay, B. P.; Lee, C. H. *Angew. Chem., Int. Ed.* **2008**, *47*, 5038–5042. (e) Berryman, O. B.; Sather, A. C.; Hay, B. P.; Meisner, J. S.; Johnson, D. W. *J. Am. Chem. Soc.* **2008**, *130*, 10895–10897.
- (10) Katayev, E. A.; Ustyuyuk, Y. A.; Sessler, J. L. *Coord. Chem. Rev.* **2006**, *250*, 3004–3037, and references therein.
- (11) See Supporting Information.
- (12) Alderighi, L.; Gans, P.; Ienco, A.; Peters, D.; Sabatini, A.; Vacca, A. *Coord. Chem. Rev.* **1999**, *184*, 311–318.
- (13) (a) Vander Griend, D. A.; Bediako, D. K.; DeVries, M. J.; DeJong, N. A.; Heeringa, L. P. *Inorg. Chem.* **2008**, *47*, 656–662. (b) Li, Y.; Vander Griend, D. A.; Flood, A. H. *Supramol. Chem.* **2009**, In press.
- (14) Hirose, K. In *Analytical Methods in Supramolecular Chemistry*; Schalley, C. A., Ed.; Wiley-VCH: Weinheim, Germany, 2007.
- (15) Scatchard, G. *Ann. N.Y. Acad. Sci.* **1949**, *51*, 660–672.

JA8077329